

Accepted for publication in *Astrophysics and Space Science*

Electrostatic Potentials in Supernova Remnant Shocks

Matthew G. Baring and Errol J. Summerlin

*Department of Physics and Astronomy MS-108,
Rice University, P.O. Box 1892, Houston, TX 77251, U.S.A.
baring@rice.edu, xerex@rice.edu*

ABSTRACT

Recent advances in the understanding of the properties of supernova remnant shocks have been precipitated by the *Chandra* and XMM X-ray Observatories, and the HESS Atmospheric Čerenkov Telescope in the TeV band. A critical problem for this field is the understanding of the relative degree of dissipative heating/energization of electrons and ions in the shock layer. This impacts the interpretation of X-ray observations, and moreover influences the efficiency of injection into the acceleration process, which in turn feeds back into the thermal shock layer energetics and dynamics. This paper outlines the first stages of our exploration of the role of charge separation potentials in non-relativistic electron-ion shocks where the inertial gyro-scales are widely disparate, using results from a Monte Carlo simulation. Charge density spatial profiles were obtained in the linear regime, sampling the inertial scales for both ions and electrons, for different magnetic field obliquities. These were readily integrated to acquire electric field profiles in the absence of self-consistent, spatial readjustments between the electrons and the ions. It was found that while diffusion plays little role in modulating the linear field structure in highly oblique and perpendicular shocks, in quasi-parallel shocks, where charge separations induced by gyrations are small, and shock-layer electric fields are predominantly generated on diffusive scales.

1. Introduction

The understanding of the character of shells and interiors of supernova remnants (SNRs) has been advanced considerably by groundbreaking observations by the *Chandra* X-ray Observatory. These have been enabled by its spectral resolution coupled with its impressive angular resolution. Of particular interest to the shock acceleration and cosmic ray physics

communities is the observation of extremely narrow non-thermal X-ray spatial profiles in selected remnants (see Long et al. 2003 for SN1006; Vink & Laming 2003 for Cas A; and Ellison & Cassam-Chenai 2005, for theoretical modeling), which define strong brightness contrasts between the shell, and the outer, upstream zones. If the synchrotron mechanism is responsible for this non-thermal emission, the flux ratios from shock to upstream indicate strong magnetic field enhancement near the shock. These ratios considerably exceed values expected for hydrodynamic compression at the shocked shell, so proposals of magnetic field amplification (e.g. Lucek & Bell 2000) in the upstream shock precursor have emerged.

Another striking determination by *Chandra* concerns electron heating by ions in the shock layer. Dynamical inferences of proton temperatures in remnant shocks can be made using proper motion studies of changes in a remnant’s angular size, or more direct spectroscopic methods (e.g. Ghavamian et al. 2003). In the case of remnant 1E 0101.2-7129, Hughes et al. (2000) used a combination of ROSAT and Chandra data spanning a decade to deduce an expansion speed. Electron temperatures T_e are determined using ion line diagnostics (assuming the equilibration $T_e = T_p$), via both the widths and relative strengths for different ionized species. From these two ingredients, Hughes et al. (2000) observed that deduced proton temperatures were considerably cooler, i.e. $3kT_p/2 \ll m_p(3u_{1x}/4)^2/2$, than would correspond to standard heating for a strong hydrodynamic shock with an upstream flow speed of u_{1x} . The same inference was made by Decourchelle et al. (2000) for Kepler’s remnant, and by Hwang et al. (2002) for Tycho’s SNR. This property is naturally expected in the nonlinear shock acceleration scenario that is widely used in describing cosmic ray and relativistic electron generation in SNRs: the highest energy particles tap significant fractions of the total available energy, leading to a reduction in the gas temperatures. This nonlinear hydrodynamic modification has been widely discussed in the cosmic ray acceleration literature (e.g. see Jones & Ellison 1991; Berezhko & Ellison 1999, and references therein), and has been extensively applied to multiwavelength SNR spectral models (e.g. see Baring et al. 1999; Berezhko et al. 2002; Ellison & Cassam-Chenai 2005; Baring, Ellison & Slane 2005).

The extent of equilibration between electrons and ions in SNR shell shocks needs to be understood, and can potentially be investigated by laboratory plasma experiments. A critical ingredient is the electrostatic coupling between electrons and protons in the shock layer, which offers the potential for considerable heating of e^- , coupled with cooling of protons, setting $m_p(3u_{1x}/4)^2/2 \gg 3kT_e/2 \gg m_e(3u_{1x}/4)^2/2$ with $T_e \neq T_p$. Probing this coupling is the subject of this paper. Here we describe preliminary results from our program to explore electrostatic energy exchange between these two species in SNR shocks, using a Monte Carlo simulation of charged particle transport, their spatial distribution and associated electric field generation. The goal is to eventually obtain a simulation with self-consistent feedback between the charge separation potentials, and the Lorentz force they impose on the charges.

The research progress outlined here indicates that the role of diffusion in quasi-parallel shocks is very important, and can readily influence computed charge separation potentials.

2. Shock Layer Electrostatics in Supernova Remnants

Cross-shock electrostatic potentials arise in the shock layer because of the different masses of electrons and ions: upstream thermal ions gyrate on larger scales than do their electron counterparts when they transit downstream of the shock for the first time. In shocks where the field is oblique to the shock normal by some angle Θ_{Bn1} upstream (and therefore a greater angle downstream), on average, protons will be located further downstream of the shock than electrons. This naturally establishes an electric field \mathbf{E} , to which the plasma responds by accelerating electrons and slowing down ions to short out the induced \mathbf{E} . A feedback loop ensues, mediated by fields and currents that vary spatially on the order of, or less than, the ion inertial scale, which is typically shorter than the ion gyroradius in astrophysical shocks such as those associated with supernova remnant shells.

Particle-in-cell (PIC) simulations are a natural technique (e.g. see Forslund & Friedberg 1971 for an early implementation) for exploring signatures of such electrostatics in shock layers. These trace particle motion and field fluctuations, obtained as self-consistent solutions of the Newton-Lorentz and Maxwell's equations, in structured zones or cells in spatially-constrained boxes. Such simulations have been used recently to probe the Weibel instability at weakly-magnetized, perpendicular, relativistic pair plasma shocks (see Silva et al. 2003; Hededal et al. 2004; Nishikawa et al. 2005). They have also been used by Shimada & Hoshino (2000) to treat electrostatic instabilities at non-relativistic, quasi-parallel electron-ion shocks. Rich in their turbulence information, due to their intensive CPU requirements, such simulations have difficulty in modeling realistic m_p/m_e mass ratios, and fully exploring 3D shock physics such as diffusive transport. Moreover, they cannot presently address the wide range of particle momenta and spatial/temporal scales encountered in the acceleration process; they often do not obtain time-asymptotic states for the particle distributions.

Monte Carlo techniques provide an alternative method that can easily resolve electron and proton inertial scales, treat fully 3D transport and large dynamical ranges in spatial and momentum scales, all at modest computation cost. While they parameterize the effects of turbulence via diffusive mean free paths (e.g. see Jones & Ellison 1991), they can accurately describe the microphysics of cross-shock electrostatic potentials. This simulational approach has been well-documented in the literature (e.g. Jones & Ellison 1991; Ellison, Jones & Baring 1996), with definitive contributions to the study of heliospheric shock systems, cosmic ray production, SNR applications and gamma-ray bursts. It models the convection and

diffusion of gyrating particles in spatially-structured flows and fields, with transport back and forth across the shock effecting diffusive Fermi-type acceleration directly from the thermal population. The mean free path λ is usually prescribed as some increasing function of particle momentum p or gyroradius r_g . Here we use this approach, with $\lambda \propto p$ adopted as a broadly representative situation: see Baring et al. (1997) for a discussion of evidence from observations and plasma simulations in support of such a specialization. Here, $\lambda/r_g = 5$ is chosen for illustrative purposes, to begin to investigate electrostatic influences on thermal and low-energy non-thermal particles in non-relativistic electron-ion shocks of arbitrary Θ_{Bn1} . Clearly then, the diffusive scales for protons and electrons are disparate by their mass ratio.

In the Monte Carlo simulation, the shock is defined magnetohydrodynamically, consisting of laminar, uniform flows and fields upstream and downstream of a sharp, planar discontinuity. The magnetic fields and flow velocities either side of the shock are related uniquely through the standard Rankine-Hugoniot solutions for energy and momentum flux conservation (e.g. see Boyd & Sanderson 1969). These solutions include essential elements of Maxwell's equations, such as the divergenceless nature of the \mathbf{B} field. In the reference frames of the local upstream and downstream fluids, the mean electric field is assumed to be zero, a consequence of very effective Debye screening, so that the only electric fields present in shock rest frames are $\mathbf{u} \times \mathbf{B}$ drift fields. The charged electrons and protons (more massive ions are omitted in this paper to simplify the identification of the principal effects) are treated as test particles, convecting into and through the shock, initially with the prescribed upstream fluid velocity \mathbf{u}_1 . This neutral beam is entirely thermal, and moreover is in equipartition, so that it has an input temperature $T_e = T_p$. The charges constantly diffuse in space to mimic collisions with magnetic turbulence that is putatively present in the shock environs, and in so doing, can be accelerated. These non-thermal particles form a minority of the total population, and provide only a minor contribution to the fields illustrated in this paper.

The charges transiting the shock distribute their downstream density in a manner that couples directly to their gyration motion (e.g. see Baring 2006), and the local densities of electrons and protons can easily be tracked in the Monte Carlo technique by accumulating “detection” data at various distances from the shock. Monte Carlo simulation runs clearly exhibit non-zero charge excursions within a proton gyroradius of the shock, an effect similar to those found in PIC codes. For example, a cold, neutral $e - p$ upstream beam develops an electron concentration near the shock in the downstream region, with protons distributed on their larger inertial scales. The resulting charge distributions $\rho(x)$ depend on both the upstream field obliquity Θ_{Bn1} , and also on the sonic Mach number $\mathcal{M}_s \approx u_{1x}/\sqrt{5kT_p/(3m_p)}$ in situations where the upstream beam is warm. Due to the steady-state, planar nature of the simulation, these distributions depend only on the coordinate x along the shock normal. It is straightforward using Gauss' law for electrostatics, $\nabla \cdot \mathbf{E} = 4\pi\rho(x)$, to integrate the

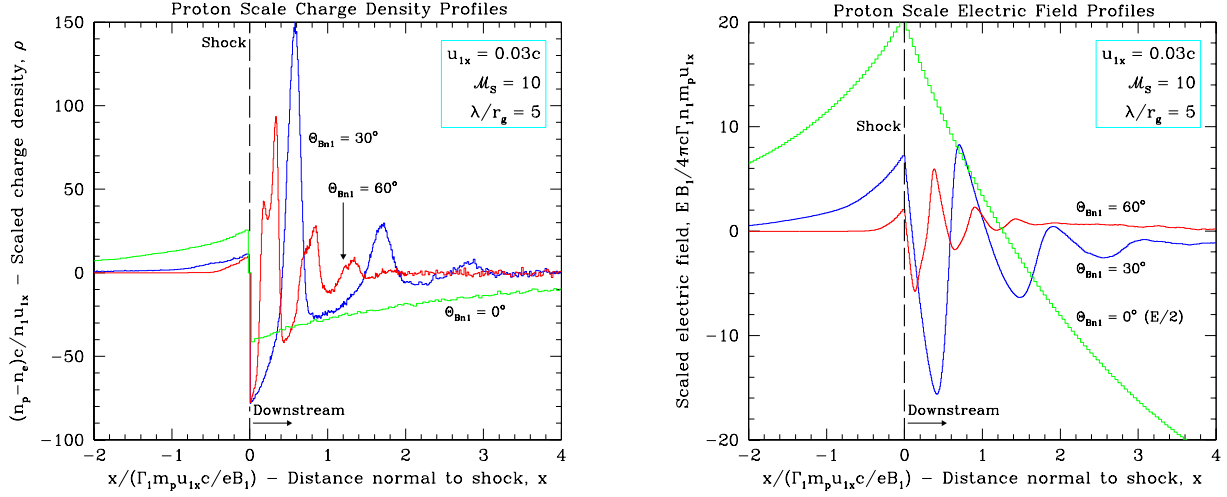


Fig. 1.— Electrostatic profiles for an electron-proton plasma shock of speed $u_{1x} = 9000$ km/sec and sonic Mach number $M_s = 10$, with upstream field obliquities $\Theta_{Bn1} = 0^\circ$ (green), $\Theta_{Bn1} = 30^\circ$ (blue) and $\Theta_{Bn1} = 60^\circ$ (red), as labelled. *Left panel:* scaled charge density distribution $\rho(x)$; *Right Panel:* resulting “*linear*” electric field profile $E \equiv E_x(x)$ computed by solving Gauss’ Law (the $\Theta_{Bn1} = 0^\circ$ displays $E_x(x)/2$). The profiles are exhibited on proton gyroscopes $r_{g,p} = m_p u_{1x} c / e B_1$, so that fluctuations on electron gyroscopes are collapsed into the shock layer (dashed vertical line). The panels display both oscillations associated with proton gyrations in oblique cases, and diffusive upstream “*precursors*,” which are most prominent when $\Theta_{Bn1} = 0^\circ$ (a parallel shock).

charge distribution profile to obtain $E_x(x) = -\partial\Phi/\partial x$. Eventually, such “*linear*” fields will then be used to compute the energy exchange between electrons and ions as they cross the non-monotonic charge separation potential $\Phi(x)$.

Linear determinations of electrostatic spatial profiles are shown in Figure 1 to illustrate the key features; these did not self-consistently include the acceleration of electrons and protons in the produced **E** field. The left panel depicts large charge density fluctuations that trace ion gyration in the downstream magnetic field. Similar fluctuations of opposite sign are created by electrons, but on much smaller scales that are not resolved in the Figure. Accordingly, “*striped*” zones of positive and negative charge density result, and this electrostatic analog of a plasma oscillation integrates to produce the **E** fields in the right panel that can accelerate or decelerate electrons and protons. The outcome depends on the shock obliquity Θ_{Bn1} when $\Theta_{Bn1} \lesssim 60^\circ$, whereas quasi-perpendicular shocks with $\Theta_{Bn1} \gtrsim 60^\circ$ possess profiles fairly close to the $\Theta_{Bn1} = 60^\circ$ case depicted in Figure 1, since they all have field obliquities $\Theta_{Bn2} \approx 80^\circ - 90^\circ$ downstream. Note also, that while the gyrotrional contributions are prominent, there is also a diffusive contribution, manifested as an upstream *precursor* modification to $\rho(x)$ and **E**. This is particularly marked in the parallel shock ($\Theta_{Bn1} = 0^\circ$)

case, where the diffusive scale along the field achieves a maximal component orthogonal to the shock plane. This diffusive influence originates in accelerated particles returning to the upstream side of the shock ($x < 0$), enhancing the density there before convecting downstream again: protons effect this on larger scales, and so control the precursors seen in the Figure (i.e. $\rho(x) > 0$ for $x < 0$). Since the fields are established on the scale of a proton gyroradius, their magnitude scales as $E_x \sim 4\pi\rho r_{g,p} = 4\pi e n_p (m_p u_{1x} c / e B_1)$, so that $|E_x/B_1| \sim 4\pi n_p m_p u_{1x} c / B_1^2 \equiv \mathcal{M}_A^2 (c/u_{1x}) \gg 1$ for Alfvénic Mach numbers $\mathcal{M}_A > 1$.

The competition between gyrokinetic and diffusive influences on electrostatics is a principal conclusion of this paper, defining a dichotomy delineating quasi-parallel and quasi-perpendicular shocks. The Monte Carlo technique can accurately trace both influences, while comfortably resolving the disparate scales for the e - p shock problem. Since the “linear” results illustrated need to be upgraded to account for the **E**-field’s influence on e^- and p motions, it is presently unclear whether ions can energize electrons overall (the right panel of the Figure suggests they may even decelerate them), and how the net work done depends on field obliquity. A noticeable feature of the electric field profiles in Fig. 1 is that for $\Theta_{Bn1} \lesssim 60^\circ$, these linear field calculations do not establish $|\mathbf{E}| \rightarrow 0$ asymptotically as $|x| \rightarrow \infty$, as required by net charge neutrality. The next step of this program will be to solve the Newton-Lorentz equation of motion $d\mathbf{p}/dt = q(\mathbf{E} + \mathbf{v} \times \mathbf{B}/c)$ to determine both drift and accelerative contributions to the charges’ motions. These will necessitate a recomputation of the **E** field profiles, and a feedback loop will result, with shock layer currents generating magnetic field excursions via Ampère’s law, $\nabla \times \mathbf{B} = 4\pi \mathbf{J}/c$. This iterative process will continue to convergence (establishing $|\mathbf{E}| \rightarrow 0$ as $|x| \rightarrow \infty$), with relaxation to equilibrium occurring on the spatial response scale u_{1x}/ω_p , where $\omega_p = \sqrt{4\pi e^2 n_p / m_p}$ is the proton plasma frequency. Since $u_{1x}/(\omega_p r_{g,p}) \sim u_{1x}/(c \mathcal{M}_A) \ll 1$, this response scale is far less than a proton gyroradius for typical SNR environmental parameters, and indeed for any strong, non-relativistic astrophysical shock.

The degree of electron energization in the cross shock potential may offer significant insights into the well-known electron injection problem at non-relativistic shocks. Electrons do not resonantly interact with Alfvén waves until they become relativistic. Levinson (1992) suggested that e^- interaction with a presumably abundant supply of whistler waves could effect pre-injection into diffusive acceleration processes, if electrons could achieve energies in excess of around 10 keV to access the whistler resonance branch. The planned self-consistent extension of the developments outlined here will help determine whether this channel of access to continued acceleration is opened up by shock layer electrostatics. Moreover, crafted laboratory plasma experiments might cast light on this aspect of shock layer physics.

3. Conclusion

In this paper, charge density and associated cross-shock electric field spatial profiles are presented for different magnetic field obliquities. It was found that in highly oblique and perpendicular shocks diffusion plays little role in modulating the field structure, which is controlled by the magnetic kinking and compression on the downstream side of the shock. In contrast, in quasi-parallel shocks, where the gyration charge separation is small, diffusion scales upstream and downstream of the shock dominate the generation of shock-layer electric fields. This is an interesting twist, suggesting that observationally, thermal X-ray emission could be distinctly different in portions of an SNR rim that establish quasi-parallel and quasi-perpendicular shocks. The work discussed here paves the way for self-consistent determination of the acceleration/deceleration of electrons and protons, their spatial distributions, and the electric fields normal to non-relativistic shocks. This development will impact the understanding of electron injection and acceleration in shocks of all obliquities.

References:

Baring, M. G. 2006, on-line proceedings of the 2006 KITP/UCSB conference “Supernova and Gamma-Ray Burst Remnants” [http://online.kitp.ucsb.edu/online/grb_c06/baring/]

Baring, M. G., Ellison, D. C., Reynolds, S. P., Grenier, I. A., & Goret, P. 1999, ApJ, 513, 311.

Baring, M. G., Ellison, D. C., & Slane, P. O. 2005, Adv. Space. Res., 35, 1041.

Baring, M. G., Ogilvie, K. W., Ellison, D. C., & Forsyth, R. J. 1997, ApJ, 476, 889.

Berezhko, E. G. & Ellison, D. C. 1999, ApJ, 526, 385.

Berezhko, E. G., Ksenofontov, L. T. & Völk, H. J. 2002, ApJ, 395, 943.

Boyd, T. J. M. & Sanderson, J. J. 1969, *Plasma Dynamics*, (Nelson & Sons, London)

Decourchelle, A., Ellison, D. C. & Ballet, J. 2000, ApJ, 543, L57.

Ellison, D. C., Baring, M. G. & Jones, F. C. 1996, ApJ, 473, 1029.

Ellison, D. C. & Cassam-Chenai, G. 2005, ApJ, 632, 920.

Forslund, D. W. & Freidberg, J. P. 1971, Phys. Rev. Lett. 27, 1189.

Ghavamian, P., Rakowski, C. E., Hughes, J. P. & Williams, T. B. 2003, ApJ, 590, 833.

Hedeland, C. B., Haugbolle, T., Frederiksen, J. T. & Nordlund, A. 2004, ApJ, 617, L107.

Hughes, J. P., Rakowski, C. E., & Decourchelle, A. 2000, ApJ, 543, L61.

Hwang, U., et. al. 2002, ApJ, 581, 110.

Jones, F. C. & Ellison, D. C. 1991, Space Science Rev., 58, 259.

Levinson, A. 1992, ApJ, 401, 73.

Long, K. S., et al. 2003, ApJ, 586, 1162.

Lucek, S. G. & Bell, A. R. 2000, M.N.R.A.S., 314, 65.

Nishikawa, K.-I., et al. 2005, ApJ, 622, 927.

Shimada, N. & Hoshino, M. 2000, ApJ, 543, L67.

Silva, L. O., et al. 2003, ApJ, 596, L121.

Vink, J. & Laming, J. M. 2003, ApJ, 584, 758.